ACS APPLIED MATERIALS & INTERFACES

Research Article

www.acsami.org

Large-Scale Growth of Well-Aligned SiC Tower-Like Nanowire Arrays and Their Field Emission Properties

Lin Wang,[†,‡] Chengming Li,[†] Yang Yang,[‡] Shanliang Chen,[‡] Fengmei Gao,[‡] Guodong Wei,*[,‡] and Weiyou Yang*[,‡]

[†]School of Materials Science and Engineering, University of Science & Technology Beijing, Beijing City, 100083, P.R. China

[‡]Institute of Materials, Ningbo University of Technology, Ningbo City, 315016, P.R. China

ABSTRACT: Fabrication of well-aligned one-dimensional (1D) nanostrucutres is critically important and highly desired since it is the key step to realize the patterned arrays to be used as the display units. In the present work, we report the large-scale and well-aligned growth of *n*-type SiC nanowire arrays on the *6H*-SiC wafer substrates via pyrolysis of polymeric precursors assisted by Au catalysts. The obtained *n*-type SiC nanowires are highly qualified with sharp tips and numerous sharp corners around the wire bodies, which bring the emitters excellent field emission (FE) performance with low turn-on fields (1.50 V/μm), low threshold fields (2.65 V/μm), and good current emission stabilities (fluctuation <3.8%). The work abilities of the *n*-type SiC tower-like nanowire arrays under high-temperature harsh environments have been investigated, suggesting that the resultant field emitters could be well serviced up to 500 °C. The temperature-enhanced FE behaviors could be attributed to the reduction of the work function induced by the rise of temperatures and the incorporated N dopants. It is believed that the present well-aligned *n*-type SiC tower-like nanowire arrays could meet nearly all stringent requirements for an ideal FE emitter with excellent FE properties, making their applications very promising in displays and other electronic nanodevices.

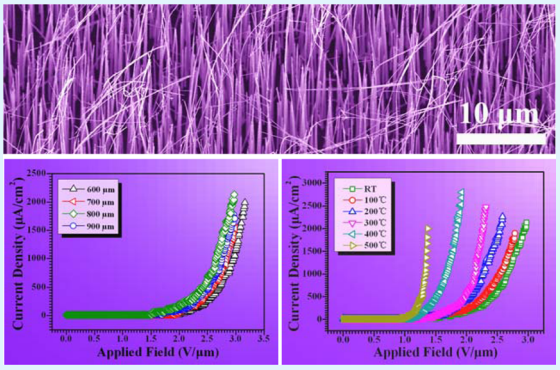

KEYWORDS: *polymeric precursors, pyrolysis, SiC, nanoarrays, doping, field emission*

1. INTRODUCTION

Over the past decades, the nanostructured semiconductor field emission (FE) cathodes have been extensively investigated, owing to their promising and interesting applications in flat-panel displays, electron microscopes, vacuum microelectronic devices, and so on.[1−4] Due to their superior mechanical properties, low thermal expansion coefficient, high thermal conductivity, excellent chemical stability, and low electron affinity,[5−7] silicon carbide (SiC) one-dimensional (1D) nanostructures are thus considered as an ideal candidate for FE application.[4,8] To date, many efforts have been devoted to making SiC 1D nanostructures in various morphologies with low turn-on fields (E_{to}, defined as the electric field required to produce a current density of 10 μA/cm^2), such as nanorods (13−17 V/μm),[9] nanobelts (3.2 V/μm),[10] nanoneedles (1.3−3.51 V/μm),[11,12] and nanowires (1.2−2.9 V/μm),[13,14] showing their excellent FE performances.

For practical FE applications, the fabrication of well-aligned 1D nanostrucutres is critically important and highly desired since it is the key step to realize the patterned SiC arrays to be used as the display units.[15−17] There are mainly two strategies for realizing the growth of SiC nanoarrays. One is defined as the "top-down" route. For example, Kang et al. reported the preparation of porous SiC nanoarrays with the E_{to} of 4.4−9.6 V/μm by electrochemical and ion etching of SiC wafers.[18] The other is the so-called the "bottom-up" route, which exhibits the advantage for the time and cost saving as compared to the former one. For example, Li et al. synthesized large-area oriented SiC nanowire arrays by chemical vapor reaction assisted by anodic aluminum oxide templates;[19] Kim et al. reported the growth of SiC nanoarrays on Si substrates using a catalytic reaction in a methane-hydrogen atmosphere;[20] Niu et al. reported the aligned growth of SiC nanowires by a thermal evaporation of ZnS and carbon on the silicon wafers;[21] Wang et al. reported the growth of SiC nanoarrays on the *6H*-SiC substrates;[22] Krishnan et al. reported the growth of SiC nanoarrays on the *4H*-SiC wafers by chemical vapor deposition;[23] Yang et al. synthesized the oriented SiC porous nanowire arrays with the E_{to} of 2.3−2.9 V/μm by *in situ* carbonizing aligned Si nanowire arrays;[13] and Pan et al. prepared the oriented SiC nanowires with the E_{to} of 0.7−1.5 V/μm by reacting SiO with aligned carbon nanotubes as the templates.[8] However, even though numerous efforts have been devoted to the growth of SiC nanoarrays, there still remains a ground challenge for preparation of SiC field emitters with desired sharp tips and suitable dopants based on the local field

Received: September 29, 2014
Accepted: December 15, 2014
Published: December 15, 2014

DOI: 10.1021/am506678x
ACS Appl. Mater. Interfaces 2015, 7, 526−533

Scheme 1. Schematic Illustration for the Growth of *n*-Type SiC Tower-Like Nanowire Arrays on the Substrate of *6H*-SiC Wafers and the FE Property Measurements

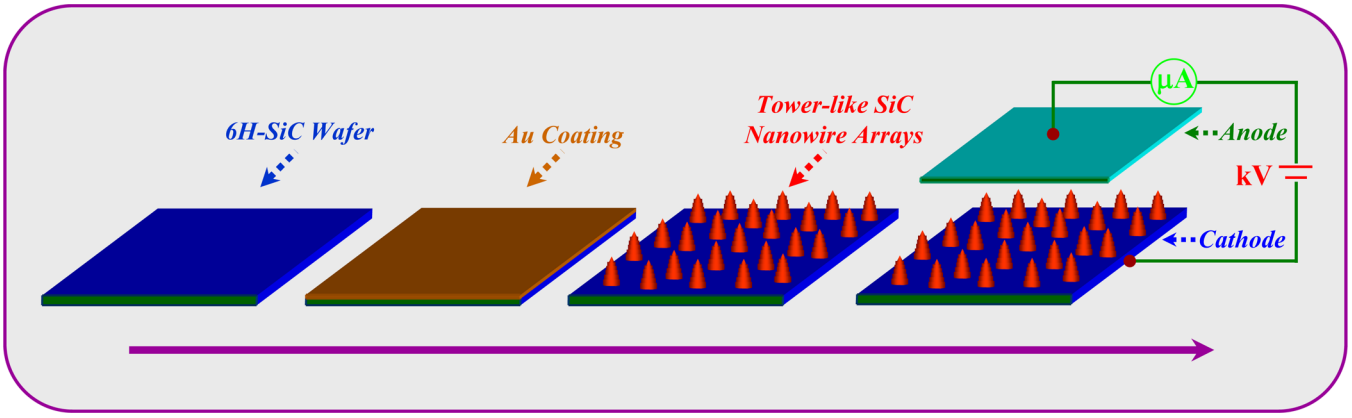

enhancement effect and doping-enhanced electron emission. Meanwhile, few works have shed light on their work abilities of the SiC emitters under high temperatures once they fall into micro/nanoscale dimensions.

Here, we report the growth of *n*-type SiC nanowire arrays via pyrolysis of the polymeric precursor on the single-crystalline *6H*-SiC wafer substrates. We mainly focus on the following important topics to offer the SiC field emitters with enhanced electron emission abilities based on the Fowler–Nordheim (F–N) theory:[24] (i) the large-scale growth of well-aligned SiC nanowire arrays; (ii) making the SiC nanowires be tapered with sharp tips and sharp corners around the wire bodies (i.e., tower-like structures); and (iii) incorporated N dopants into the SiC nanowires, leading to the formation of *n*-type SiC nanoarrays for enhanced FE performances. The FE measurements suggest that the E_{to} values of as-synthesized *n*-type SiC nanowire arrays ranged from 1.50 to 0.94 V/μm with the temperatures raised from room temperature (RT) to 500 °C, suggesting their very promising application in field emission displays.

2. EXPERIMENTAL PROCEDURE

n-Type SiC nanowire arrays were synthesized by catalyst-assisted pyrolysis of polymeric precursor polyureasilazane (PSN, Ceraset, Kion Corporation, USA) on the *6H*-SiC wafer substrate, which is shown in Scheme 1 with the following FE measurements. In a typical experimental process, the polymeric precursor of PSN was first solidified by heat treatment at 260 °C for 30 min under Ar atmosphere and then subjected to ball milling into fine powders. Subsequently, *6H*-SiC(0001) wafers (1 × 1 cm^2) were sprayed with Au (90 nm thickness) used as the catalyst for the growth of SiC nanowire arrays. The obtained fine powders were then put into the bottom of a high-purity graphic crucible (99%), and the SiC wafers were located over the powders with a fixed distance to the powder surface of ~2 cm. The crucible with a graphic paper cover was then placed into a graphite-heater furnace. The furnace chamber was first pumped to 10^{-4} pa, and then the N_2/Ar gas mixture (0.1 MPa, N_2:Ar = 5:95, volume percent, both N_2 and Ar are 99.99% purity) was introduced into the chamber with a flowing rate of 200 sccm for the following pyrolysis procedure. The gas purge was repeated three times to reduce the O_2 content to a negligible level. Finally, the furnace was heated to the desired temperature of 1500 °C in 60 min and maintained there for 20 min, followed by furnace cooling to the ambient temperature.

The obtained products were characterized by using field emission scanning electron microscopy (FESEM, S-4800, Hitachi, Japan) and transmission electron microscopy (TEM, JEM-2100F, JEOL, Japan) equipped with energy-dispersive X-ray spectroscopy (EDX, Quantax-STEM, Bruker, Germany). The FE properties were measured in a home-built high vacuum field emission setup with a base pressure of ~1.5 × 10^{-7} Pa at the temperatures ranging from RT to 500 °C. The current–voltage (I–V) curves were recorded on a Keithley 248 unit with a detection resolution of 0.1 fA. The distances between the surface of samples and the anode in the vacuum chamber were typically fixed at 600–900 μm.

3. RESULTS AND DISCUSSION

The obtained products were first observed under SEM. Figure 1(a) shows a typical SEM image under a low magnification,

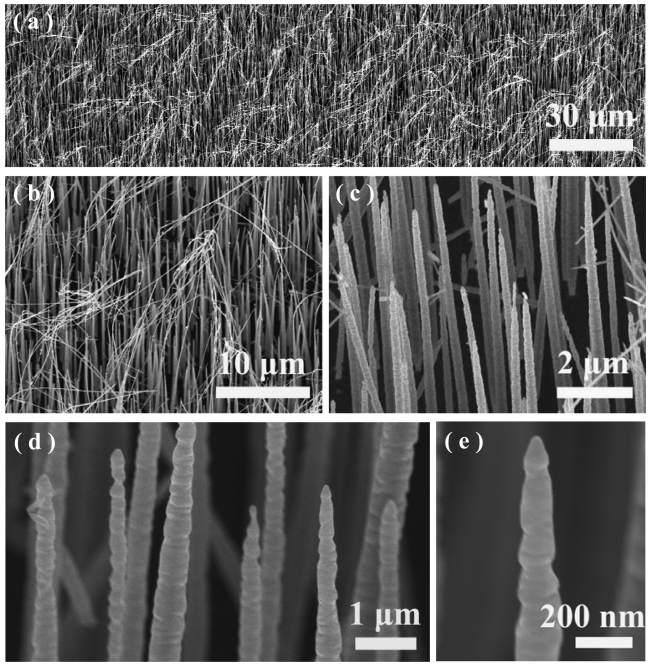

Figure 1. (a–d) Typical SEM images of the as-synthesized *n*-type SiC nanowire arrays under different magnifications. (e) A typical enlarged SEM image showing the details of the wire tip.

revealing that the wire-like products entirely and uniformly cover the whole SiC wafer substrate (area: 1 cm^2). Figure 1(b,c) displays the as-grown products under higher magnifications. On the basis of the SEM observations, the average number density of SiC nanowire arrays is ca. ~5.7 × 10^5 nanowires/mm^2. It seems that the nanowires are highly oriented, leading to the growth of well-aligned nanowire arrays. The average length of the wires is ~10 μm. Notably, the

DOI: 10.1021/am506678x
ACS Appl. Mater. Interfaces 2015, 7, 526–533

nanowires have the unique morphology features with small roots, tapered bodies, and sharp tips, which make them in a typically tower-like shape. As we know, for the growth of the nanowires dominated by the typical vapor−liquid−solid (VLS) mechanism, the diameters of the wires are often confined by the sizes of the liquid catalysts.[25] That is to say, the smaller diameters of the wires could be obtained with a smaller sized catalytic droplet. In the present work, the growth of SiC nanowires with small roots, tapered bodies, and sharp tips could be attributed to the following cases. At the early stage, the size of the SiC crystal nucleus is small. The large contact angle between the nuclei and the catalytic droplet is expected to generate an outward force on the nanostructures.[26] Thus, the droplet cannot effectively confine the lateral growth of the wire at the early stage, resulting in the growth of the nanowires with an increasing diameter (i.e., the formation of the roots). With the growth of the wire along the lateral direction, the contact area between the wire and the catalytic droplet increases, leading to the decrease of the contact angle and the outward force. Consequently, the lateral growth is effectively confined by the catalytic droplet, making the followed growth of nanowires with relatively constant diameters.[25] The subsequent growth of the SiC naowires with tapered bodies and sharp tips could be ascribed to the following reasons. The dissolutions of the Si and C elements in Au catalytic droplets are remarkably influenced by the variation of the temperatures. This means that a decrease of the temperature might result in a lower dissolution of the vapor species within the catalytic liquid droplet, which, in turn, leads to the decrease of the catalytic droplet sizes. That is to say, with the decrease of the temperatures, the sizes of the liquid Au catalytic droplets would be gradually reduced, which consequently causes the growth of the SiC with tapered bodies and sharp tips.[11,25,27,28] Notably, all of the nanowires have sharp tips with numerous sharp corners around the wire bodies (Figure 1(d,e)). According to the local field enhancement effect, these sharp tips and sharp corners could bring a significant enhancement to the electron emission of the as-synthesized nanowires,[29] making them an ideal candidate as the field emitters.

The characterizations of the obtained products were further performed by TEM. For the TEM sample preparation, the nanowires were scratched and detached from the SiC wafer substrate, followed by ultrasonic treatment in alcohol for 10 min. Then a drop of the resultant solutions was dripped onto the copper grid. Figure 2(a) shows a typical TEM image of a single nanowire under a low magnification, suggesting that the nanowire possesses a needle-like shape with a tapered structure and rough surface. Figure 2(b) is the corresponding enlarged TEM image, showing the detailed characteristics of the tip of the nanowire. It seems that the tip is clear and typically sized at ∼10 nm (the inset Figure 2(b)). Figure 2(c) shows a representative TEM image of the wire body. It discloses that numerous sharp corners existed around the body of the as-synthesized nanowire, as shown by the white dashed arrow heads in Figure 2(c). Figure 2(d) is a typical HRTEM image recorded from the marked area of A in (b), clarifying its single crystalline nature of the resultant nanowires. The interplanar fringes can be clearly observed, and the spacing between two set of fringes is ∼0.25 nm, agreeing with the (111) crystal faces of 3C-SiC. The top left inset is the corresponding SAED pattern, which can be indexed to the 3C-SiC structure (JCPDS Card No. 41-0360). It is identical over the entire nanowire, confirming its single-crystalline nature. The results of the TEM,

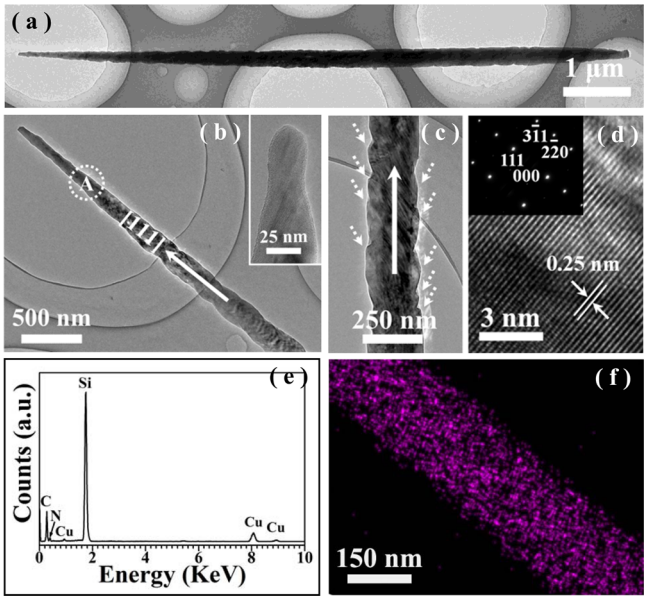

Figure 2. (a) Typical TEM image of a single nanowire under a low magnification. (b) Typical TEM image of the wire tip under a high magnification. The inset shows the sharp and clear tips of the nanowire with a typical diameter of ∼10 nm. (c) A representative TEM image of the wire, showing numerous sharp corners existing around the wire body. (d) A typical HRTEM image recorded from the marked area of A in (b). The inset is the corresponding SAED pattern. (e) A representative EDX spectrum of the nanowires. (f) A typical element mapping of N dopants within the SiC nanowires.

HRTEM, and SAED pattern suggest that the wires grow along the [111] direction, as indicated by the arrowhead marked in Figure 2(a). The chemical compositions of the SiC nanowires are identified by EDX under TEM, revealing that they consist mainly of Si, C, N, and Cu (Figure 2(e)). The Cu signals come from the copper grid used to support the TEM sample. The atomic ratio of Si to C, within the experimental limit, is close to 1:1, suggesting the nanostructure is SiC. Figure 2(f) presents the typical mapping of the N elements within the SiC nanowires, suggesting their uniform spatial distribution with an average concentration of 3.01 at.%. On the basis of our previous work,[12,30] the as-synthesized products are *n*-type SiC nanowire arrays.

Figure 3(a) shows the emission current density (J) versus the applied electric field (E) curves (J−E) of the as-synthesized *n*-type SiC nanowire arrays with anode−cathode separation distance (d) fixed at 800 μm under RT. J and E can be calculated from the total emission current (I) divided by the effective area (S) and the external voltage applied (V) divided by the anode−cathode separation distance (d), respectively. The curve reveals that the dependence of the emission current density on the applied field is exponential-like after a certain value. The relatively smooth and consistent curve implies the stable electron emission. The corresponding F−N curve (shown as the top left inset, plotted in the $\ln(J/E^2) - 1/E$ relationship) exhibits an approximately linear relationship, suggesting that the electron emission from the *n*-type SiC nanoarrays follows the conventional field emission mechanism. Figure 3(b) shows the changes of the FE properties of the *n*-type SiC nanoarrays with the distances ranging from 600 to 900 μm, suggesting that all curves show a similar tendency. The E_{to} and threshold field (E_{thr}, defined to be the electric field required to produce a current density of 1 mA/cm^2) are in the range of

DOI: 10.1021/am506678x
ACS Appl. Mater. Interfaces 2015, 7, 526−533

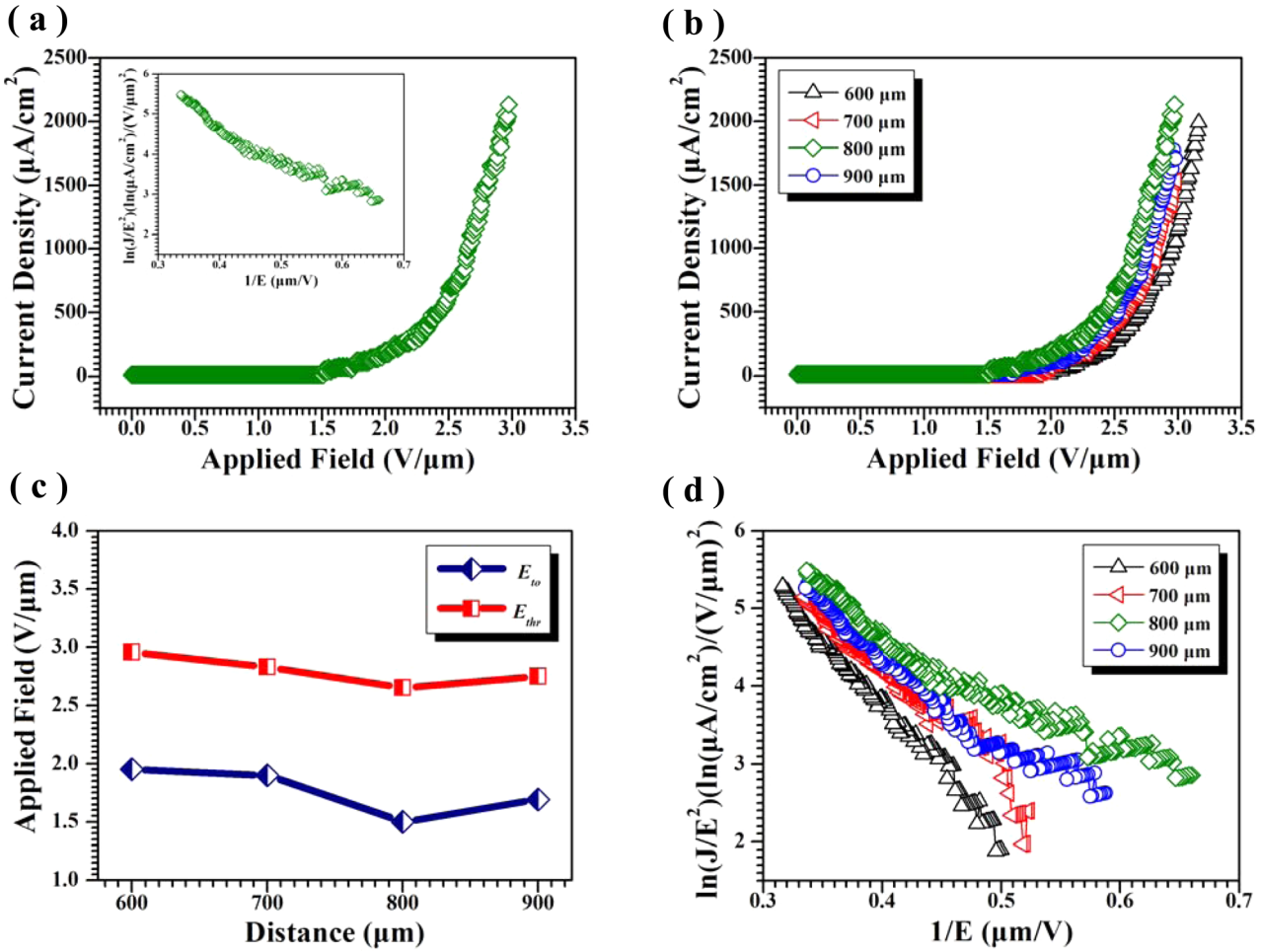

Figure 3. (a) Typical J–E curve of the n-type SiC nanowire arrays with the anode–cathode separation distance fixed at 800 μm under RT. The inset is the corresponding F–N plot. (b) Typical J–E curves of the SiC nanoarrays with the distances fixed at 600–900 μm under RT. (c) The variations of E_{to} and E_{thr} with the distances. (d) The corresponding F–N plots under different distances.

1.50–1.95 V/μm and 2.65–2.96 V/μm (Figure 3(c)), respectively. While the d is set as 800 μm, the best FE properties with the E_{to} and E_{thr} of 1.50 V/μm and 2.65 V/μm could be reached, respectively. The E_{to} is superior to those of most reported works for SiC nanostructures with different morphologies[9,10,12,13] which always fall in ~2–17 V/μm range and other inorganic semiconductor nanoarrays such as ZnO nanoarrays (2.4–4.6 V μm^{-1}),[31] AlN nanorod arrays (E_{to}, 3.8 V μm^{-1}),[32] and CdS nanowire arrays (12.2 V/μm).[33] Regardless of the various d fixed between the cathode and anode, it seems that the electron emissions from the n-type SiC nanoarrays all obey the conventional field emission mechanism (Figure 3(d)). On the basis of the reported work function of SiC (4.0 eV) under RT[4] and the slope (m) of the F–N plot at d = 800 μm, the field enhancement factor β can be calculated to be ~4482 at RT. This high β can be mainly attributed to the special morphology of nanowires with a high aspect ratio and small radii of curvature.

The current emission stability of the emitters is another key parameter to concern their device applications. We employ J_{drop} (i.e., J degradation during the testing time) to evaluate the current emission stability of the as-fabricated nanoarrays,[34] which can be calculated by

$$J_{drop} = (J_{first} - J_{last})/J_{mean} \quad (1)$$

where J_{first}, J_{last}, and J_m refer to the first, last, and mean emission current densities, respectively. Figure 4 displays the variation of the emission current density at a current density of ~693.3 μA/cm^2 under the applied electric field of 2.5 V/μm with a monitoring time of 240 min, which are examined by

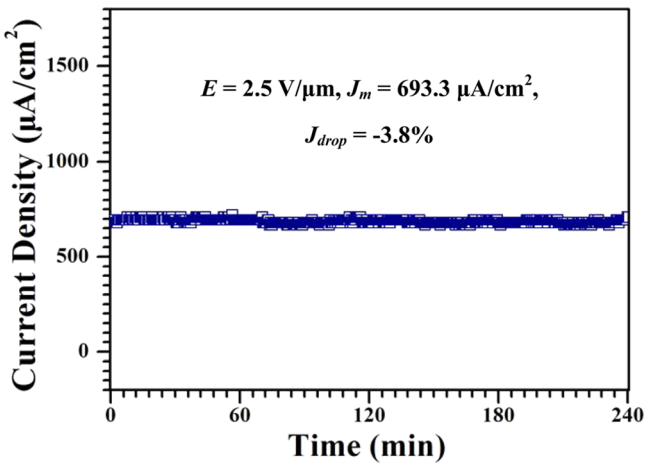

Figure 4. FE emission stability of the n-type SiC tower-like nanowire arrays under RT.

DOI: 10.1021/am506678x
ACS Appl. Mater. Interfaces 2015, 7, 526–533

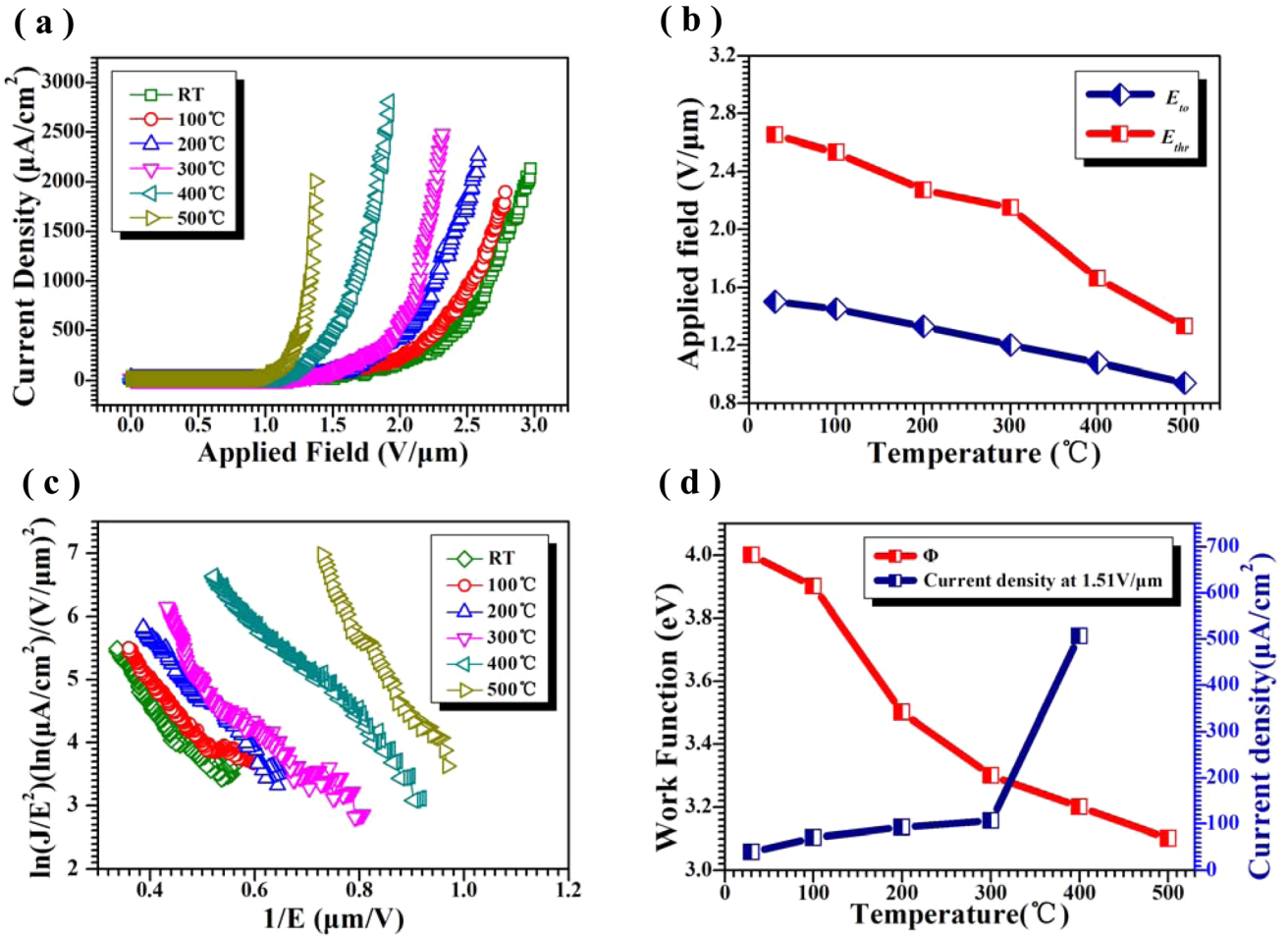

Figure 5. (a) J–E plots of n-type SiC nanowire arrays under different temperatures ranging from RT to 500 °C. (b) The variations of E_{to} and E_{thr} with the changes of the temperatures. (c) The corresponding F–N plots of SiC nanoarrays under different temperatures. (d) The variations of Φ and the current densities at 1.51 V/μm with the changes of the temperatures.

automatically recording the emission currents at every 3 s under RT. A very small current fluctuation <3.8% can be observed, suggesting the highly stable electron emission of our synthesized n-type SiC nanoarrays. It is much more stable than most of the other SiC nanostructures and inorganic semiconductor nanoarrays.[13,35] For example, Zhang et al. reported that the current fluctuation of tungsten oxide nanowire arrays was ~5%;[36] Das et al. reported that the current fluctuation of CuO nanostrucutres was ~5%;[37] and Yang et al. reported that the current fluctuation of B-doped SiC nanowires was ~14%.[29]

As compared to the Si semiconductors, the unique and significant advantage of SiC counterparts is to be serviced in harsh environments (e.g., high temperatures). However, how about the work abilities of the SiC emitters under high temperatures once they fall into micro/nanodimensions? Few works have focused on this point. To disclose the field emission behavior of the present n-type SiC nanoarrays under high temperatures, the FE performances were measured in the temperature range of RT to 500 °C. Figure 5(a) shows the curves (J–E) of the as-synthesized n-type SiC nanowire arrays under different temperatures with a fixed d of ~800 μm. All the relatively smooth and consistent curves indicate their stable electron emission, suggesting that the present n-type SiC nanoarrays could be well serviced under the high-temperature harsh environments up to 500 °C. Figure 5(b) presents the variations of the E_{to} and E_{thr} with the change of the temperatures. It suggests that, when increasing the temperature from RT to 500 °C, the E_{to} and E_{thr} of the n-type SiC nanoarrays decrease from 1.50 to 0.94 and 2.65 to 1.33 V/μm, respectively, implying that the electron emission of the present n-type nanoarrays is sensitive to the temperatures.

To understand the FE behaviors of the n-type SiC nanoarrays working under different temperatures, the field emission J–E characteristics were analyzed using the Fowler–Nordheim (F–N) equation[24]

$$J = (A\beta^2E^2/\Phi)\exp[-B\Phi^{3/2}(\beta E)^{-1}] \quad (2)$$

where E is the applied electric field; $A = 1.54 \times 10^{-6}$ A eV V^{-2}; $B = 6.83 \times 10^3$ eV$^{-3/2}$ V μm^{-1}; Φ is the work function of the emitter material; and β is the field-enhanced factor. The corresponding F–N curves, plotted as $\ln(J/E^2) - 1/E$, are presented in Figure 5(c). The slopes of all F–N plots show the approximately linear relationships, indicating that the FE of the n-type SiC nanoarrays from RT to 500 °C obeys the F–N rule. With respect to the fact that there is no significant influence of temperature (RT to 500 °C) on the crystal structure of SiC nanostructures,[38] the β should be determined only by the emitter geometry and thus can be considered as a constant regardless of the temperature variations. Determining of the Φ can trace the F–N plots, whose slope k can be calculated by

DOI: 10.1021/am506678x
ACS Appl. Mater. Interfaces 2015, 7, 526–533

$$k = -B\Phi^{3/2}/\beta \quad (3)$$

Then the work functions of *n*-type SiC nanonarray emitters under different temperatures can be calculated out,[39] which show a decrease from 4.0 to 3.1 eV with the temperature increased from RT to 500 °C (shown as the red plot in Figure 5(d)). The reduced Φ is responsible for the observed thermo-enhanced FE behaviors.[40,41] The inherent mechanism can be ascribed to the increase of the electron−hole pairs induced by the rise of the temperatures.[42−44] For *n*-type semiconductors, the electrons at the top of the valence band can transit to the bottom of the conduction band with a higher energy and larger probability caused by the increased temperatures, leading to the generation of more electron−hole pairs. The increased electrons could take part in the current transport, which consequently results in the decreased resistance and a better FE performance.[45,46] It can be confirmed that the electron emission could be enhanced significantly from 40.0 to 506.7 $\mu A/cm^2$ (at 1.51 V/μm) upon the temperatures increase from RT to 400 °C, as shown by the blue plot in Figure 5(d).

The excellent FE properties of the as-synthesized *n*-type SiC tower-like nanowire arrays can be mainly ascribed to the following issues: (i) The well-aligned and tapered structures with clear and sharp tips of the as-grown nanowires (Figure 1 (d and e)).[4,11,31,47−51] These sharp tips with small curvature radius could facilitate the electron emission significantly due to the local field enhancement effect.[52] The clear tips of our wires (the top right inset in Figure 2(b)) also benefit from the electron emission because the alloy drops covered on the emitter tips could bring an additional energy barrier to limit the electron emission.[1,53−55] (ii) The unique tower-like morphology of the as-fabricated SiC nanowires, which could offer the wires with numerous sharp corners around the bodies.[56,57] These sharp corners could also act as the efficient electron emission sites due to the local field enhancement effect.[11,29] That is to say, the unique tower-like structure could significantly increase the density of the emitting sites and thus makes a profound improvement on the FE of the nanostructures. (iii) The incorporated N dopants within the SiC nanowires.[12,35,58,59] The N dopants could favor a more localized impurity state near the conduction band edge, which thus could make the Fermi level be shifted toward the vacuum and lead to the reduction of Φ. (iv) The outstanding intrinsic properties of SiC materials with high mechanical strength and chemical stability, which allow the SiC nanoarray emitters to be well-serviced under high temperatures up to 500 °C.[5−7] In brief, these unique features as mentioned above suggest that our well-aligned *n*-type SiC tower-like nanowire arrays could meet nearly any stringent requirement for an ideal FE emitter with excellent FE performances, making their very promising applications in displays and other electronic nanodevices.

4. CONCLUSIONS

In summary, we have demonstrated the large-scale and well-aligned growth of *n*-type SiC nanowire arrays on the 6*H*-SiC wafer substrates via pyrolysis of polymeric precursors with Au as the catalysts. The obtained SiC nanowires are highly qualified with sharp tips and numerous sharp corners around the wire bodies as well as 3.01 at. % incorporated N dopants. The FE characteristics show that E_{to} and E_{thr} of the as-synthesized *n*-type SiC tower-like nanowire arrays are 1.50−1.95 and 2.65−2.96 V/μm with the changes of the anode−cathode separation distances from 600 to 900 μm, respectively, showing that the *n*-type SiC nanoarray emitters possess very excellent FE properties. Their current emission fluctuation under RT is measured to be of 3.8%, suggesting they have a high electron emission stability. The field enhancement factor is calculated to be ∼4482 at RT. The investigation on the FE performance under high temperatures discloses that the E_{to} is reduced from 1.50 to 0.94 V/μm with the temperature raised from RT to 500 °C, implying that the as-synthesized *n*-type SiC nanoarray emitters could be serviced under harsh environments up to 500 °C. The temperature-enhanced FE behaviors could be attributed to the reduction of the work function induced by the rise of temperatures and the incorporated N dopants. Current work suggests our *n*-type SiC tower-like nanowire arrays could be an excellent candidate for field emitters.

AUTHOR INFORMATION

Corresponding Authors

*E-mail: wgd588@163.com (G. Wei).

*E-mail: weiyouyang@tsinghua.org.cn (W. Yang). Tel.: +86-574-87080966. Fax: +86-574-87081221.

Notes

The authors declare no competing financial interest.

ACKNOWLEDGMENTS

The work was supported by the 973 program (Grant No. 2012CB326407), National Natural Science Foundation of China (NSFC, Grant Nos. 51372122, 51372123, and 51202115), and Foundation of Educational Commission in Zhejiang Province of China (Grant no. Y201327895).

REFERENCES

(1) De Heer, W. A.; Chatelain, A.; Ugarte, D. A Carbon Nanotube Field-Emission Electron Source. *Science* **1995**, *270*, 1179−1180.

(2) Wu, Z.; Deng, S.; Xu, N.; Chen, J.; Zhou, J.; Chen, J. Needle-Shaped Silicon Carbide Nanowires: Synthesis and Field Electron Emission Properties. *Appl. Phys. Lett.* **2002**, *80*, 3829−3831.

(3) Lee, C.; Lee, T.; Lyu, S.; Zhang, Y.; Ruh, H.; Lee, H. Field Emission From Well-Aligned Zinc Oxide Nanowires Grown at Low Temperature. *Appl. Phys. Lett.* **2002**, *81*, 3648−3650.

(4) Fang, X.; Bando, Y.; Gautam, U. K.; Ye, C.; Golberg, D. Inorganic Semiconductor Nanostructures and Their Field-Emission Applications. *J. Mater. Chem.* **2008**, *18*, 509−522.

(5) Casady, J.; Johnson, R. Status of Silicon Carbide (SiC) as a Wide-Bandgap Semiconductor for High-Temperature Applications: A Review. *Solid-State Electron.* **1996**, *39*, 1409−1422.

(6) Wong, E. W.; Sheehan, P. E.; Lieber, C. M. Nanobeam Mechanics: Elasticity, Strength, and Toughness of Nanorods and Nanotubes. *Science* **1997**, *277*, 1971−1975.

(7) Fan, J.; Wu, X.; Chu, P. Low-Dimensional SiC Nanostructures: Fabrication, Luminescence, and Electrical Properties. *Prog. Mater. Sci.* **2006**, *51*, 983−1031.

(8) Pan, Z.; Lai, H. L.; Au, F. C.; Duan, X.; Zhou, W.; Shi, W.; Wang, N.; Lee, C. S.; Wong, N. B.; Lee, S. T. Oriented Silicon Carbide Nanowires: Synthesis and Field Emission Properties. *Adv. Mater.* **2000**, *12*, 1186−1190.

(9) Zhou, X.; Lai, H.; Peng, H.; Au, F. C.; Liao, L.; Wang, N.; Bello, I.; Lee, C.; Lee, S. Thin β-SiC Nanorods and Their Field Emission Properties. *Chem. Phys. Lett.* **2000**, *318*, 58−62.

(10) Wei, G.; Qin, W.; Kim, R.; Sun, J.; Zhu, P.; Wang, G.; Wang, L.; Zhang, D.; Zheng, K. Quantum Confinement Effect and Field Emission Characteristics of Ultrathin 3*C*-SiC Nanobelts. *Chem. Phys. Lett.* **2008**, *461*, 242−245.

(11) Wei, G.; Liu, H.; Shi, C.; Gao, F.; Zheng, J.; Wei, G.; Yang, W. Temperature-Dependent Field Emission Properties of 3C-SiC Nanoneedles. *J. Phys. Chem. C* **2011**, *115*, 13063−13068.

DOI: 10.1021/am506678x
ACS Appl. Mater. Interfaces 2015, 7, 526−533

(12) Chen, S.; Ying, P. Z.; Wang, L.; Wei, G.; Zheng, J.; Gao, F.; Su, S.; Yang, W. Growth of Flexible N-Doped SiC Quasialigned Nanoarrays and Their Field Emission Properties. *J. Mater. Chem. C* **2013**, *1*, 4779−4784.
(13) Yang, Y.; Meng, G.; Liu, X.; Zhang, L.; Hu, Z.; He, C.; Hu, Y. Aligned SiC Porous Nanowire Arrays with Excellent Field Emission Properties Converted from Si Nanowires on Silicon Wafer. *J. Mater. Chem. C* **2008**, *112*, 20126−20130.
(14) Wu, R.; Zhou, K.; Wei, J.; Huang, Y.; Su, F.; Chen, J.; Wang, L. Growth of Tapered SiC Nanowires on Flexible Carbon Fabric: Toward Field Emission Applications. *J. Mater. Chem. C* **2012**, *116*, 12940−12945.
(15) Musa, I.; Munindrasdasa, D.; Amaratunga, G.; Eccleston, W. Ultra-Low-Threshold Field Emission from Conjugated Polymers. *Nature* **1998**, *395*, 362−365.
(16) Kong, J.; Soh, H. T.; Cassell, A. M.; Quate, C. F.; Dai, H. Synthesis of Individual Single-Walled Carbon Nanotubes on Patterned Silicon Wafers. *Nature* **1998**, *395*, 878−881.
(17) Xu, S.; Wei, Y.; Kirkham, M.; Liu, J.; Mai, W.; Davidovic, D.; Snyder, R. L.; Wang, Z. L. Patterned Growth of Vertically Aligned ZnO Nanowire Arrays on Inorganic Substrates at Low Temperature without Catalyst. *J. Am.. Chem. Soc.* **2008**, *130*, 14958−14959.
(18) Kang, M. G.; Lezec, H. J.; Sharifi, F. Stable Field Emission from Nanoporous Silicon Carbide. *Nanotechnology* **2013**, *24*, 065201.
(19) Li, Z. J.; Zhang, J. L.; Meng, A.; Guo, J. Z. Large-Area Highly-Oriented SiC Nanowire Arrays: Synthesis, Raman, and Photoluminescence Properties. *J. Phys. Chem. B* **2006**, *110*, 22382−22386.
(20) Kim, H. Y.; Park, J.; Yang, H. Direct Synthesis of Aligned Silicon Carbide Nanowires from the Silicon Substrates. *Chem. Commun.* **2003**, 256−257.
(21) Niu, J. J.; Wang, J. N. A Simple Route to Synthesize Scales of Aligned Single-Crystalline SiC Nanowires Arrays with Very Small Diameter and Optical Properties. *J. Phys. Chem. B* **2007**, *111*, 4368−4373.
(22) Wang, H.; Lin, L.; Yang, W.; Xie, Z.; An, L. Preferred Orientation of SiC Nanowires Induced by Substrates. *J. Mater. Chem. C* **2010**, *114*, 2591−2594.
(23) Krishnan, B.; Thirumalai, R. V. K.; Koshka, Y.; Sundaresan, S.; Levin, I.; Davydov, A. V.; Merrett, J. N. Substrate-Dependent Orientation and Polytype Control in SiC Nanowires Grown on *4H*-SiC Substrates. *Cryst. Growth Des.* **2011**, *11*, 538−541.
(24) Fowler, R. H.; Nordheim, L. Electron Emission in Intense Electric Fields. *Proc. R. Soc. London, Ser. A* **1928**, *119*, 173−181.
(25) Wang, H.; Xie, Z.; Yang, W.; Fang, J.; An, L. Morphology Control in the Vapor-Liquid-Solid Growth of SiC Nanowires. *Cryst. Growth Des.* **2008**, *8*, 3893−3896.
(26) Ross, F. M.; Tersoff, J.; Reuter, C. M. Sawtooth Faceting in Silicon Nanowires. *Appl. Phys. Lett.* **2005**, *95*, 146104.
(27) Chen, S.; Ying, P.; Wang, L.; Gao, F.; Wei, G.; Zheng, J.; Xie, Z.; Yang, W. Controlled Growth of SiC Flexible Field Emitters with Clear and Sharp Tips. *RSC Adv.* **2014**, *4*, 8376−8382.
(28) Feng, W.; Ma, J.; Yang, W. Precise Control on the Growth of SiC Nanowires. *CrystEngComm* **2012**, *14*, 1210−1212.
(29) Yang, Y.; Yang, H.; Wei, G.; Wang, L.; Shang, M.; Yang, Z.; Tang, B.; Yang, W. Enhanced Field Emission of *p*-type 3C-SiC Nanowires with B Dopants and Sharp Corners. *J. Mater. Chem. C* **2014**, *2*, 4515−4520.
(30) He, Z.; Wang, L.; Gao, F.; Wei, G.; Zheng, J.; Cheng, X.; Tang, B.; Yang, W. Synthesis of *n*-type SiC Nanowires with Tailored Doping Levels. *CrystEngComm* **2013**, *15*, 2354−2358.
(31) Zhao, Q.; Zhang, H.; Zhu, Y.; Feng, S.; Sun, X.; Xu, J.; Yu, D. Morphological Effects on the Field Emission of ZnO Nanorod Arrays. *Appl. Phys. Lett.* **2005**, *86*, 203115.
(32) He, J. H.; Yang, R.; Chueh, Y. L.; Chou, L. J.; Chen, L. J.; Wang, Z. L. Aligned AlN Nanorods with Multi-Tipped Surfaces-Growth, Field-Emission, and Cathodoluminescence Properties. *Adv. Mater.* **2006**, *18*, 650−654.
(33) Zhai, T.; Fang, X.; Bando, Y.; Liao, Q.; Xu, X.; Zeng, H.; Ma, Y.; Yao, J.; Golberg, D. Morphology-Dependent Stimulated Emission and Field Emission of Ordered CdS Nanostructure Arrays. *ACS Nano* **2009**, *3*, 949−959.
(34) Deng, J. H.; Zheng, R. T.; Zhao, Y.; Cheng, G. A. Vapor-Solid Growth of Few-Layer Graphene Using Radio Frequency Sputtering Deposition and Its Application on Field Emission. *ACS Nano* **2012**, *6*, 3727−3733.
(35) Zhang, X.; Chen, Y.; Liu, W.; Xue, W.; Li, J.; Xie, Z. Growth of *n*-type 3C-SiC Nanoneedles on Carbon Fabric: Toward Extremely Flexible Field Emission Devices. *J. Mater. Chem. C* **2013**, *1*, 6479−6486.
(36) Zhang, X.; Gong, L.; Liu, K.; Cao, Y.; Xiao, X.; Sun, W.; Hu, X.; Gao, Y.; Chen, J.; Zhou, J. Tungsten Oxide Nanowires Grown on Carbon Cloth as a Flexible Cold Cathode. *Adv. Mater.* **2010**, *22*, 5292−5296.
(37) Das, S.; Saha, S.; Sen, D.; Ghorai, U. K.; Banerjee, D.; Chattopadhyay, K. K. Highly Oriented Cupric Oxide Nanoknife Arrays on Flexible Carbon Fabric as High Performing Cold Cathode Emitter. *J. Mater. Chem. C* **2014**, *2*, 1321−1330.
(38) Mah, T.; Hecht, N. L.; McCullum, D. E.; Hoenigman, J. R.; Kim, H. M.; Katz, A. P.; Lipsitt, H. A. Thermal Stability of SiC Fibres (Nicalon). *J. Mater. Sci.* **1984**, *19*, 1191−1201.
(39) Fransen, M. J.; Van Rooy, T. L.; Kruit, P. Field Emission Energy Distributions From Individual Multiwalled Carbon Nanotubes. *Appl. Surf. Sci.* **1999**, *146*, 312−327.
(40) Lee, S. H.; Lee, D. H.; Lee, W. J.; Kim, S. O. Tailored Assembly of Carbon Nanotubes and Graphene. *Adv. Funct. Mater.* **2011**, *21*, 1338−1354.
(41) Lyth, S.; Hatton, R.; Silva, S. Efficient Field Emission from Li-Salt Functionalized Multiwall Carbon Nanotubes on Flexible Substrates. *Appl. Phys. Lett.* **2007**, *90*, 013120.
(42) Da Silva, A. F.; Pernot, J.; Contreras, S.; Sernelius, B. E.; Persson, C.; Camassel, J. Electrical Resistivity and Metal-Nonmetal Transition in *n*-type Doped *4H*-SiC. *Phys. Rev. B* **2006**, *74*, 245201.
(43) Kim, K. J.; Lim, K. Y.; Kim, Y. W.; Kim, H. C. Temperature Dependence of Electrical Resistivity (4−300 K) in Aluminum- and Boron- Doped SiC Ceramics. *J. Am. Ceram. Soc.* **2013**, *96*, 2525−2530.
(44) Chen, J.; Deng, S.; Xu, N.; Zhang, W.; Wen, X.; Yang, S. Temperature Dependence of Field Emission from Cupric Oxide Nanobelt Films. *Appl. Phys. Lett.* **2003**, *83*, 746−748.
(45) Li, J.; Chen, J.; Shen, B.; Yan, X.; Xue, Q. Temperature Dependence of the Field Emission from the Few-Layer Graphene Film. *Appl. Phys. Lett.* **2011**, *99*, 163103.
(46) She, J.; Xiao, Z.; Yang, Y.; Deng, S.; Chen, J.; Yang, G.; Xu, N. Correlation between Resistance and Field Emission Performance of Individual ZnO One-Dimensional Nanostructures. *ACS Nano* **2008**, *2*, 2015−2022.
(47) Xu, N.; Huq, S. E. Novel Cold Cathode Materials and Applications. *Mater. Sci. Eng., R* **2005**, *48*, 47−189.
(48) Wei, A.; Sun, X. W.; Xu, C. X.; Dong, Z. L.; Yu, M. B.; Huang, W. Stable Field Emission from Hydrothermally Grown ZnO Nanotubes. *Appl. Phys. Lett.* **2006**, *88*, 213102.
(49) Fang, X.; Bando, Y.; Ye, C.; Shen, G.; Gautam, U. K.; Tang, C.; Golberg, D. Si Nanowire Semisphere-Like Ensembles as Field Emitters. *Chem. Commun.* **2007**, 4093−4095.
(50) Zeng, H.; Xu, X.; Bando, Y.; Gautam, U. K.; Zhai, T.; Fang, X.; Liu, B.; Golberg, D.; Template Deformation-Tailored, ZnO Nanorod/Nanowire Arrays: Full Growth Control and Optimization of Field-Emission. *Adv. Funct. Mater.* **2009**, *19*, 3165−3172.
(51) Fang, X.; Wu, L.; Hu, L. ZnS Nanostructure Arrays: A Developing Material Star. *Adv. Mater.* **2011**, *23*, 585−598.
(52) Liu, C.; Hu, Z.; Wu, Q.; Wang, X. Z.; Chen, Y.; Sang, H.; Zhu, J. M.; Deng, S. Z.; Xu, N. S. Vapor-Solid Growth and Characterization of Aluminum Nitride Nanocones. *J. Am. Chem. Soc.* **2005**, *127*, 1318−1322.
(53) Zhu, W.; Kochanski, G. P.; Jin, S. Low-Field Electron Emission from Doped Nanostructured Diamond. *Science* **1998**, *282*, 1471−1473.
(54) Murakami, H.; Hirakawa, M.; Tanaka, C.; Yamakawa, H. Field Emission from Well-Aligned, Patterned, Carbon Nanotube Emitters. *Appl. Phys. Lett.* **2000**, *76*, 1776−1779.

DOI: 10.1021/am506678x
ACS Appl. Mater. Interfaces 2015, 7, 526−533

(55) Bonard, J. M.; Salvetat, J. P.; Stöckli, T.; de Heer, W. A.; Forro, L.; Chatelain, A. Field Emission from Single-Wall Carbon Nanotube Films. *Appl. Phys. Lett.* **1998**, *73*, 918−920.
(56) Saito, Y.; Hata, K.; Murata, T. Field Emission Patterns Originating from Pentagons at the Tip of a Carbon Nanotube. *Jpn. J. Appl. Phys.* **2000**, *39*, L271.
(57) Zhang, X.; Chen, Y.; Xie, Z.; Yang, W. Shape and Doping Enhanced Field Emission Properties of Quasialigned 3C-SiC Nanowires. *J. Phys. Chem. C* **2010**, *114*, 8251−8255.
(58) You, J. B.; Zhang, X. W.; Cai, P. F.; Dong, J. J.; Gao, Y.; Yin, Z. G.; Chen, N. F.; Wang, R. Z.; Yan, H. Enhancement of Field Emission of the ZnO Film by the Reduced Work Function and the Increased Conductivity via Hydrogen Plasma Treatment. *Appl. Phys. Lett.* **2009**, *94*, 262105.
(59) Chen, S.; Ying, P. Z.; Wang, L.; Wei, G.; Zheng, J.; Gao, F.; Su, S.; Yang, W. Growth of Flexible N-Doped SiC Quasialigned Nanoarrays and Their Field Emission Properties. *J. Mater. Chem. C* **2013**, *1*, 4779.

DOI: 10.1021/am506678x
ACS Appl. Mater. Interfaces 2015, 7, 526−533